



Tsukushi is essential for the formation of the posterior semicircular canal that detects gait performance

Toru Miwa^{1,2,3} · Naofumi Ito^{4,5} · Kunimasa Ohta⁶

Received: 27 January 2021 / Accepted: 25 May 2021 / Published online: 1 June 2021
© The International CCN Society 2021

Abstract

Tsukushi is a small, leucine-rich repeat proteoglycan that interacts with and regulates essential cellular signaling cascades in the chick retina and murine subventricular zone, hippocampus, dermal hair follicles, and the cochlea. However, its function in the vestibules of the inner ear remains unknown. Here, we investigated the function of Tsukushi in the vestibules and found that Tsukushi deficiency in mice resulted in defects in posterior semicircular canal formation in the vestibules, but did not lead to vestibular hair cell loss. Furthermore, Tsukushi accumulated in the non-prosensory and prosensory regions during the embryonic and postnatal developmental stages. The downregulation of Tsukushi altered the expression of key genes driving vestibule differentiation in the non-prosensory regions. Our results indicate that Tsukushi interacts with *Wnt2b*, bone morphogenetic protein 4, fibroblast growth factor 10, and netrin 1, thereby controlling semicircular canal formation. Therefore, Tsukushi may be an essential component of the molecular pathways regulating vestibular development.

Keywords Tsukushi · Vestibule · Posterior semicircular canal · *Wnt2b* · *Bmp4* · FGF10

Introduction

Tsukushi (TSK) is a small leucine-rich repeat proteoglycan that functions as an extracellular signaling molecule in various developmental processes in vertebrates (Ahmad et al. 2018; Dellett et al. 2012; Ohta et al. 2004). The diverse functions of TSK depend on its ability to bind and interact with the intermediates of some major signaling pathways, including bone morphogenetic protein (Bmp), fibroblast growth factor (FGF), transforming growth factor-beta (Tgf- β), and Wnt (Ahmad et al. 2018; Hocking et al. 1998; Merline et al. 2009; Schaefer and Iozzo 2008). TSK reportedly affects the central nervous network development (Hossain et al. 2013; Ito et al. 2010) and wound healing (Niimori et al. 2012). It is expressed in the chick retina (Ohta et al. 2004, 2006) and mouse subventricular zone (Ito et al. 2021, in press), hippocampus (Ahmad et al. 2020; Ito et al. 2010), dermal hair follicles (Niimori et al. 2012), and the cochlea (Miwa et al. 2020). However, its function, vestibular localization, and the molecular mechanisms underlying vestibular development have not yet been investigated.

The development of the inner ear is a complex process involving the three-dimensional growth of labyrinth structures. The embryological origin of the inner ear is the ear vesicle (Langman and Sadler 2008), which is composed of a

✉ Toru Miwa
t-mwia@kitano-hp.or.jp

Naofumi Ito
mikan03orange@gmail.com

Kunimasa Ohta
ohta9203@artsci.kyushu-u.ac.jp

¹ Department of Otolaryngology-Head and Neck Surgery, Kitano Hospital, Tazuke Kofukai Medical Research Institute, Ougimaci, Kita-ku, Osaka, Japan

² Department of Otolaryngology-Head and Neck Surgery, Graduate School of Medicine, Kyoto University, Shogoin Kawahara-cho, Sakyo-ku, Kyoto, Japan

³ Department of Otolaryngology-Head and Neck Surgery, Graduate School of Medicine, Kumamoto University, Honjo, Kumamoto, Japan

⁴ Department of Developmental Neurobiology, Graduate School of Life Sciences, Kumamoto University, Honjo, Kumamoto, Japan

⁵ K.K. Sciex Japan, Shinagawa, Tokyo, Japan

⁶ Department of Stem Cell Biology, Faculty of Arts and Science, Kyushu University, Motoooka, Nishi-ku, Fukuoka, Japan

ventral part, comprising the sacculus and ductus cochlearis, and a dorsal part, called the utriculus. Three semicircular canals (SCs) develop from the growth and fusion of three flattened protuberances of the utriculus. The first step of SC formation is the appearance of a dorsal and lateral pouch (diverticula) in the otic vesicle. The dorsal pouch gives rise to the anterior and posterior canals and crus commune, and the lateral pouch gives rise to the lateral (horizontal) canal. Pouch formation and growth are driven by the rapid thinning of the dorsolateral otocyst epithelium, rather than a local increase in cell proliferation (Lang et al. 2000). Initially, a loss of epithelial morphology occurs in the side of the pouch, with a concomitant disruption of the underlying basement membrane (Martin and Swanson 1993). Cell proliferation in the periotic mesenchyme then pushes the sides of pouch together to form the fusion plate. Once the fusion plate is formed, the cells are cleared from the area by apoptosis, leaving the canal duct formed from the surrounding pouch rim. Some fusion plate cells are resorbed back into the duct epithelium (Martin and Swanson 1993), whereas other cells undergo an epithelial–mesenchymal transition (EMT) and become a part of the periotic mesenchyme. Programmed cell death has also been shown to play an important role in eliminating these cells in the chicken embryo (Fekete et al. 1997).

Previous studies have shown that the expression of the laminin-related protein NTN1 is restricted to the fusion plate, where it is required for the expression of laminin and the breakdown of the basement membrane via the proliferation of the surrounding mesenchyme, subsequently pushing the fusing epithelial sheets together (Salminen et al. 2000). NTN1 is involved in a signaling cascade leading to the local production of matrix metalloproteinases to digest basement membrane proteins. These proteases are required to remodel the extracellular matrix during morphogenesis, angiogenesis, cell migration, and axonal migration (Werb and Chin 1998). The extent of cell clearance and resorption at the fusion plate correlates with the expression of NTN1. In *Ntn1* mutants, the mitotic index is reduced in the surrounding mesenchyme, and the fusion plates fail to form (Salminen et al. 2000).

NTN1 interacts with leucine-rich repeats and immunoglobulin-like domain 3 (LRIG3) to form the lateral semicircular canal (LSC) duct, and with Distal-Less Homeobox 5 (DLX5) to form the anterior semicircular canal (ASC) and the posterior semicircular canal (PSC) (Martin and Swanson 1993; Rakowiecki and Epstein 2013). The expression of DLX5 in the rims of the ASC and PSC is dependent on a signaling cascade involving sensory-dependent extracellular Wnt, Bmp, and FGF (Chang et al. 2008; Kiernan

et al. 2006; Pauley et al. 2003; Shibata et al. 2016b; Wu and Kelley 2012). Notably, changes in the Bmp expression in the developing inner ear cause dysmorphogenesis (Li et al. 2005; Ohyama et al. 2010). As a Wnt signal inhibitor, Bmp plays a crucial role in the development of the peripheral eye and inner ear (Dellett et al. 2012; Ohta et al. 2011; Rakowiecki and Epstein 2013). Bmp also serves as an FGF signal inhibitor and is thus necessary for vestibular development (Morris et al. 2007; Uejima et al. 2010). Wnt signaling in the non-sensory epithelial integrity of the anterior and posterior canal rims is necessary to induce *Bmp4*, thereby facilitating EMT (Chang et al. 2008; Huang et al. 2009; Postigo 2003; Vervoort et al. 2010). In addition, previous studies have suggested that prolonged exposure to *Bmp4* signals is necessary for DLX5 activation in the SCs and NTN1 suppression, resulting in resorption (Chang et al. 2008). The redistribution of DLX5 and NTN1 is slightly upregulated, thereby causing fusion plate over-resorption. Furthermore, FGF10 is required to remove fused cells after semicircular plate formation, especially during PSC formation (Ohuchi et al. 2005). Bmp post-transcriptionally represses SOX2, as observed during cardiac development (Rao et al. 2016), and previous studies have shown that the loss of SOX2 induces hair cell loss. Mutant SOX2 mice have ears that lack one or more ampullae and cristae; however, the crus commune and canal ducts are present (Kiernan et al. 2005, 2006). These findings indicate a degree of independence from sensory signaling during the development of non-sensory elements of the semicircular canal system (Kiernan et al. 2005, 2006).

Tsukushi directly binds to the CRD region of Fzd4 and competes with *Wnt2b* for binding to the same domain, thereby preventing Wnt activation (Ohta et al. 2011). We hypothesized that TSK may be involved in the development of the vestibules based on its role in the development of cochlear sensory cells (Miwa et al. 2020). In this study, we investigated the expression and functions of TSK during inner ear morphogenesis and after birth, and its interaction with Bmp, whose signaling is crucial for inner ear development. We also examined SOX2 expression in the prosensory regions.

Materials and methods

Generation of a *TSK*-knockout (KO) mouse model

TSK-KO C57BL/6J mice (*Mus musculus domesticus*) were produced by inserting a LacZ/Neo cassette into the *TSK*-coding exon (Ito et al. 2010). Wild-type littermates (WT) confirmed by genotyping were used as the control group.

Heterozygous littermates identified by genotyping were used in LacZ expression experiments. The mice were housed in an air-conditioned room, maintained at approximately 25 °C and 50% humidity. The acclimatization period was 1 week. The mice were fed a standard commercial pellet diet and water ad libitum. Embryonic day 0.5 (E0.5) was designated as the day when a vaginal plug was observed at noon. All animal experiments in this study were approved by the Committee on the Use and Care of Animals of the Kumamoto University (approval number H28-053) and complied with veterinary standards.

Quantitative gait assessment

Quantitative gait assessment was performed as described previously with slight modifications (Fernagut et al. 2002). The mice were placed in 4.5 cm × 40 cm acrylic clear boxes for 20–40 s. Paw movement was recorded using an iPhone X camera (1080 p at 30 fps, Apple, Cupertino, CA, USA) from underneath and later analyzed using the freeware motion-analysis software Kinovea (version 0.8.15; Open source by Joan Charmant). Gait patterns within 5 cm of the start and 5 cm of the end of the movement were excluded because of velocity changes. Images in which the mice made stops or obvious decelerations were also excluded from the analysis. Gait parameters including stride length (cm), variability in stride length, the base of support, cadence, and average speed were measured; the results are shown in Online Resource 1 Supplementary Information.

Tissue processing

At E9.5, E11.5, E12.5, E13.5, E15.5, and postnatal day 0 (P0), embryo heads were dissected and fixed with 4% paraformaldehyde (PFA) in phosphate-buffered saline (PBS) for 12 h at 4 °C. For postnatal assessments, the mice were anesthetized by an intraperitoneal injection of 4 mg/kg xylazine (Bayer, Shawnee Mission, KS, USA) and 120 mg/kg ketamine-HCl (Daiichi Sankyo, Tokyo, Japan) in 0.9% NaCl, and were fixed by cardiac perfusion of 4% PFA in PBS. The inner ears were dissected from the temporal bones and decalcified in 0.5 M EDTA (Wako, Osaka, Japan) for 3 days at 25 °C. The cochleae were embedded in optimal cutting temperature (OCT) compound (Sakura Finetek Japan, Tokyo, Japan) and serially sectioned to 12- μ m thickness using a cryostat (Microm HM 505 E Cryostat, GMI, Ramsay, MN, USA).

B-Galactosidase staining

To investigate TSK expression, the inner ears of the mice heterozygous for LacZ insertion in *TSK* were examined at E9.5, E11.5, E13.5, E15.5, P0, and P30 by staining according to the manufacturer's instructions (X-gal Staining Assay Kit; Genlantis, San Diego, CA, USA). The slides were dried for 30 min at 25 °C, fixed with 2% glutaraldehyde for 10 min at 25 °C, and then stained with 400 mg/mL X-gal and incubated for 18 h at 37 °C. The sections were washed twice and imaged at 1360 × 1024 pixels using a BZ-9000 microscope (Keyence, Osaka, Japan) with uniform photographic exposure parameters ($n = 5$ at each stage) (Miwa et al. 2020).

Anatomical studies of the inner ear

The inner ears of mice at P30 were dissected from the temporal bones and fixed with 4% PFA in PBS for 12 h at 4 °C. The surrounding soft tissue and mastoid air cells were carefully removed using a pair of fine forceps. Sample images were captured digitally using an SMZ1500 microscope (Nikon, Tokyo, Japan) at a resolution of 1360 × 1024 pixels ($n = 5$).

Hematoxylin and eosin staining

Histological analysis was performed by Hematoxylin and eosin (HE) staining to assess gross morphology. Images were obtained using a BZ-9000 microscope ($n = 5$ for each genotype).

Immunostaining

Sections at E12.5 and E13.5 were blocked with 10% normal goat serum in PBS containing 0.1% Triton X-100 (IBI Scientific, Peosta, IA, USA) for 10 min at 25 °C and labeled using a rabbit antibody against Myosin 7a (Myo7a, #PA1-936, 1:500; Thermo Fisher Scientific, Rockford, IL, USA), a rabbit antibody against laminin (#NB300-144, 1:100; Novus, Centennial, CO, USA), a chicken antibody against netrin 1 (#NB100-1605, 1:100; Novus), a rabbit antibody against DLX5 (#ABIN6258115, 1:100; Antibodies online.com, Aachen, Germany), and a rabbit antibody against SOX2 (#14962S, 1:200; Cell Signaling, CA, USA) in a humidified chamber for 1 h at 25 °C. Subsequently, the sections were washed and incubated with secondary antibodies conjugated with Alexa Fluor 594 (1:500; Thermo Fisher Scientific, Rockford, IL, USA) and Alexa Fluor 488 (1:500; Thermo Fisher Scientific) for 1 h at 25 °C. After washing with PBS,

the tissue sections were counterstained with Hoechst 33342 (Molecular Probes, OR, USA) with the use of each antibody.

The samples were then labeled with 3,3'-diaminobenzidine tetrachloride (DAB) using the HRP-DAB Cell & Tissue Staining Kit (#CTS019; R&D, Minneapolis, MN, USA). After incubation with a sheep antibody against FGF10 (#AF6224, 1:1000, R&D) at 4 °C overnight, the slides were rinsed with PBS and incubated with labeled HRP according to the manufacturer's instructions for 30 min. Color reactions were developed using DAB chromogen solution, and all slides were counterstained with hematoxylin and imaged at 1360 × 1024 pixels, using a BZ-9000 microscope with uniform photographic exposure parameters. Sections representative of at least five mice were selected.

In situ hybridization

The cochleae collected at E13.5, E15.5, and P0 were examined by in situ hybridization with antisense riboprobes for *Wnt2b* and *Bmp4* labeled with digoxigenin using the DIG RNA Labeling Kit (Roche, Indianapolis, IN, USA). The probes were produced using the corresponding DNA constructs. Detailed protocols have been previously described (Miwa et al. 2019; Shibata et al. 2016a, b) and are available upon request. A minimum of five samples was prepared for each time point.

Quantification of vestibular hair cells

In the P30 specimens, Myo7a-positive vestibular hair cells were identified and counted in all crista ampullae (CA), macula saccule (MS), and macula utricule (MU). All counts were performed using the Cell Counter function in ImageJ (NIH) (Schneider et al. 2012).

Laser microdissection

At E13.5, whole heads were dissected and incubated with 4% PFA in PBS for 1 h at 25 °C. The samples were then embedded in OCT compound, sectioned to 10- μ m thickness along the cochlear modiolus long axis plane, mounted on uncharged slides (Leica Microsystems, Wetzlar, Germany), and dried at 25 °C. The sections were incubated in 95% acetone at -20 °C and dried at room temperature immediately before laser microdissection using an LMD7 system (Leica Microsystems) as previously described (Pagedar et al. 2006; Takeda et al. 2019). Cell samples were obtained from vestibular cells. Each slide contained

multiple adjacent sections, and all cells were pooled onto a single cap.

Quantitative reverse-transcription polymerase chain reaction

The total RNA was extracted from each sample, obtained by laser microdissection using microRNA extraction kits (Qiagen, Valencia, CA, USA), quantified using GeneQuant100 (GE Healthcare, Amersham, UK), and diluted as needed to achieve uniform concentrations. cDNA was then synthesized using the One-Step PrimeScript RT-PCR Kit (Takara Bio, Otsu, Japan) according to the manufacturer's instructions, with primers for *Wnt2b*, *Bmp4*, *Sox2*, and *GAPDH* (Applied Bionics, Foster City, CA, USA). Targets were amplified using Takara Dice TP960 over 40 cycles of denaturation at 95 °C for 15 s and annealing at 60 °C for 1 min. Relative gene expression was calculated using the standard curve method and normalized to the *GAPDH* signal.

Statistical analysis

Data are presented as mean \pm standard deviation. Two groups were compared using Mann–Whitney *U* test. Statistical analyses were performed using Microsoft Excel (Redmond, WA, USA). Results with a *P* value of < 0.05 were considered statistically significant.

Results

TSK expression in the sensory and non-sensory epithelium of the developing inner ear

To elucidate the expression pattern of *TSK* in the inner ear, embryos expressing the *lacZ* reporter gene within the coding exon of *TSK* were stained with X-gal. At E9.5 and E11.5, *TSK*-*LacZ*-expressing cells were observed in the whole epithelium of the otocyst (Fig. 1a, b). At E13.5, E15.5, and P0, they were found in the Common SC (C-SC) duct, MS, MU, PSC ampulla (PA), and LSC ampulla (LA) (Fig. 1c–e). At P30, they were detected in the C-SC duct, MS, MU, and PA (Fig. 1f). Negative controls of X-gal staining are shown in Online Resource 2 Supplementary Information.

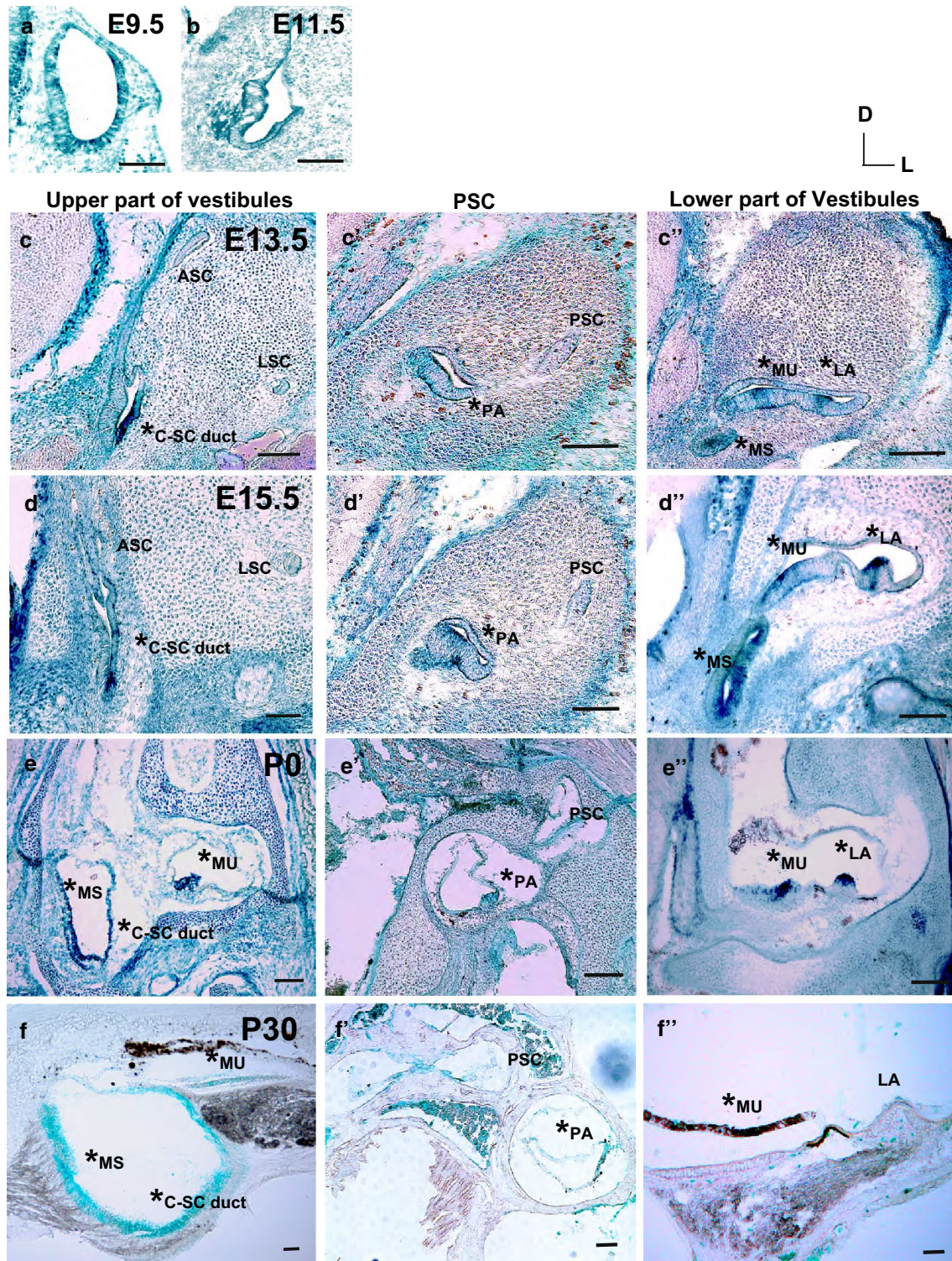


Fig. 1 Spatiotemporal expression of TSK in the inner ear of *TSK* heterozygous mice. **a, b** At E9.5 and E11.5, TSK-LacZ-expressing cells were localized in the whole epithelium of the otocyst. **c–f** Upper part of the vestibules at E13.5 (**c**), E15.5 (**d**), P0 (**e**), and P30 (**f**). TSK-LacZ-expressing cells were localized at the C-SC duct (indicated with asterisks). At P0 and P30, TSK-LacZ-expressing cells were localized at MS and MU (asterisks in **e, f**). **c'–f'** PSC levels at E13.5 (**c'**), E15.5 (**d'**), P0 (**e'**), and P30 (**f'**), with TSK-LacZ-expressing cells localized

at PA (asterisks in **c'–f'**). **c''–f''** Lower part of the vestibules at E13.5 (**c''**), E15.5 (**d''**), P0 (**e''**), and P30 (**f''**), with TSK-LacZ-expressing cells detected at MU and LA (asterisks in **c''–f''**). C-SC duct, common semicircular canal duct; ASC, anterior semicircular canal; LSC, lateral semicircular canal; MS, maculae saccule; MU, macula utricule; PSC, posterior semicircular canal; PA, posterior ampullae; LA, lateral ampullae. Scale bar: 100 μ m (**a, b**) or 50 μ m (**c–f''**)

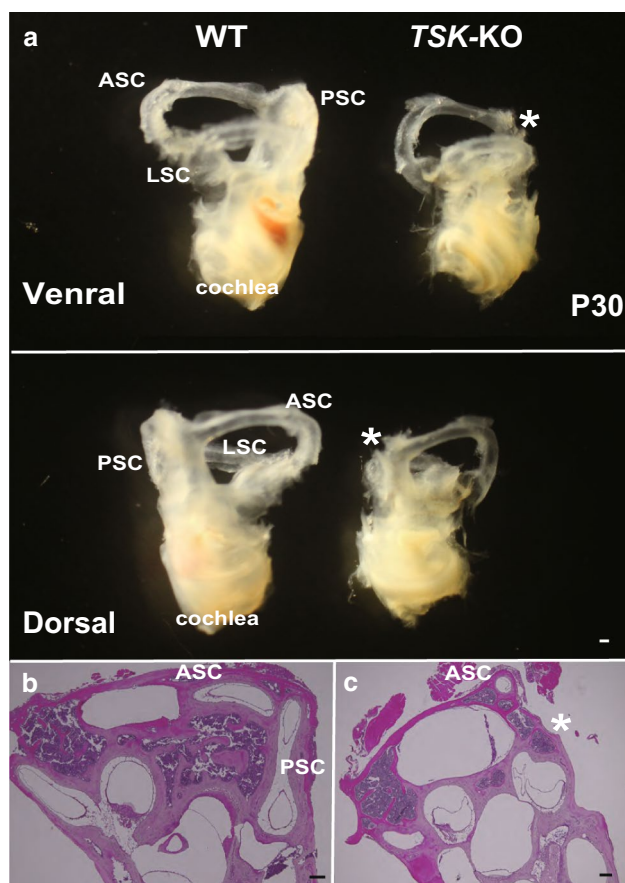


Fig. 2 Loss of TSK signaling in the vestibules caused defects in the posterior semicircular canal. **a** The cochlea in *TSK-KO* mice were smaller than that in WT mice at P30. PSC was defective in *TSK-KO* mice at P30 (indicated with asterisks). **b, c** Representative HE-stained cross-sectional images through the cochleae and vestibules in WT mice show that all three epithelial ducts were surrounded by periotic mesenchyme-derived cartilaginous cells, forming the SCs at P30. In contrast, PSC was absent in all *TSK-KO* mice (indicated with an asterisk; $n=5$). SC, semicircular canal; ASC, anterior semicircular canal; LSC, lateral semicircular canal; PSC, posterior semicircular canal. Scale bar: 100 μ m

Abnormal gait performance and a lack of posterior semicircular canal in *TSK-KO* mice

The *TSK-KO* mice exhibited a wide-based ataxic gait (Online Resource 3 Supplementary Information). As shown in Online Resource 4 Supplementary Information, the stride length, coefficient of variation (CV) of stride length, base of support, cadence, and average speed were significantly different between the WT and *TSK-KO* mice, with the WT performing better ($P < 0.001$, $P < 0.001$, $P < 0.001$, $P = 0.03$, and $P = 0.006$, respectively). To determine whether disequilibrium was associated with vestibular morphologies, we

removed the cochleae and vestibules of mice and found that the cochlea of the *TSK-KO* mice was smaller than that in the WT mice, as previously reported (Yano et al. 2017). In addition, PSC was defective in the *TSK-KO* mice (Fig. 2a). Cross-sections of the cochleae and vestibules of WT mice showed that all three epithelial ducts are surrounded by cartilaginous cells derived from the periotic mesenchyme, thus forming the SCs (Fig. 2a). In contrast, in all *TSK-KO* mice, only the anterior and lateral ducts were surrounded by a bony canal (Fig. 2b).

We found that in the vestibular sensory regions, particularly in the CA, MS, and MU, there were no significant differences in the number of hair cells between the WT and *TSK-KO* mice in any region (Fig. 3g; $P = 0.29$, $P = 0.06$, and $P = 0.48$, respectively).

TSK is required for normal fusion plate formation of posterior semicircular canal

We investigated the mechanism of vestibular development in the *TSK-KO* mice. At E12.5, in the normal mouse ear, although the epithelial wall had become thinner in the PSC outpocketing, the vestibular epithelial cells did not lose their epithelial morphology or the sharp boundary of the mesenchyme (Fig. 4a). In PSC outpocketing in *TSK-KO* mice, the fusion plate was not formed and vestibular epithelial cells were maintained (Fig. 4b). Next, we examined laminin and NTN1 expression. At E13.5, laminin expression was upregulated around the vestibular epithelium in both upper part of vestibules (Fig. 4c, d) and PSC levels (Fig. 4c', d') in the *TSK-KO* mice. At E13.5, NTN1 expression was slightly upregulated around the vestibular epithelium in the upper part of both vestibules (Fig. 4e, f) and PSC levels (Fig. 4e', f') in the *TSK-KO* mice.

TSK-KO enhanced *Wnt2b*, thinly spread *Bmp4*, and upregulated *DLX5* and *FGF10* in the non-sensory regions

To determine the cause of the non-formation of the fusion plate in *TSK-KO* vestibules, we examined the expression of *Wnt2b*, *Bmp4*, and *FGF10* at E13.5 and that of *DLX5*. *Wnt2b* was detected by in situ hybridization in the MS, LSC, ASC, PA, and PSC in WT mice (Fig. 5a). In the *TSK-KO* mice, *Wnt2b* was detected in the same regions and the C-SC duct (Fig. 5b). Finally, qRT-PCR following laser microdissection (LMD) of whole vestibule tissues revealed that *Wnt2b* mRNA expression was significantly increased in *TSK-KO* vestibules compared with that in the WT mice (Fig. 5c, $P = 0.01$). By in situ hybridization, *Bmp4* was detected in the MS, C-SC duct, LSC, ASC, PA, and PSC in WT mice

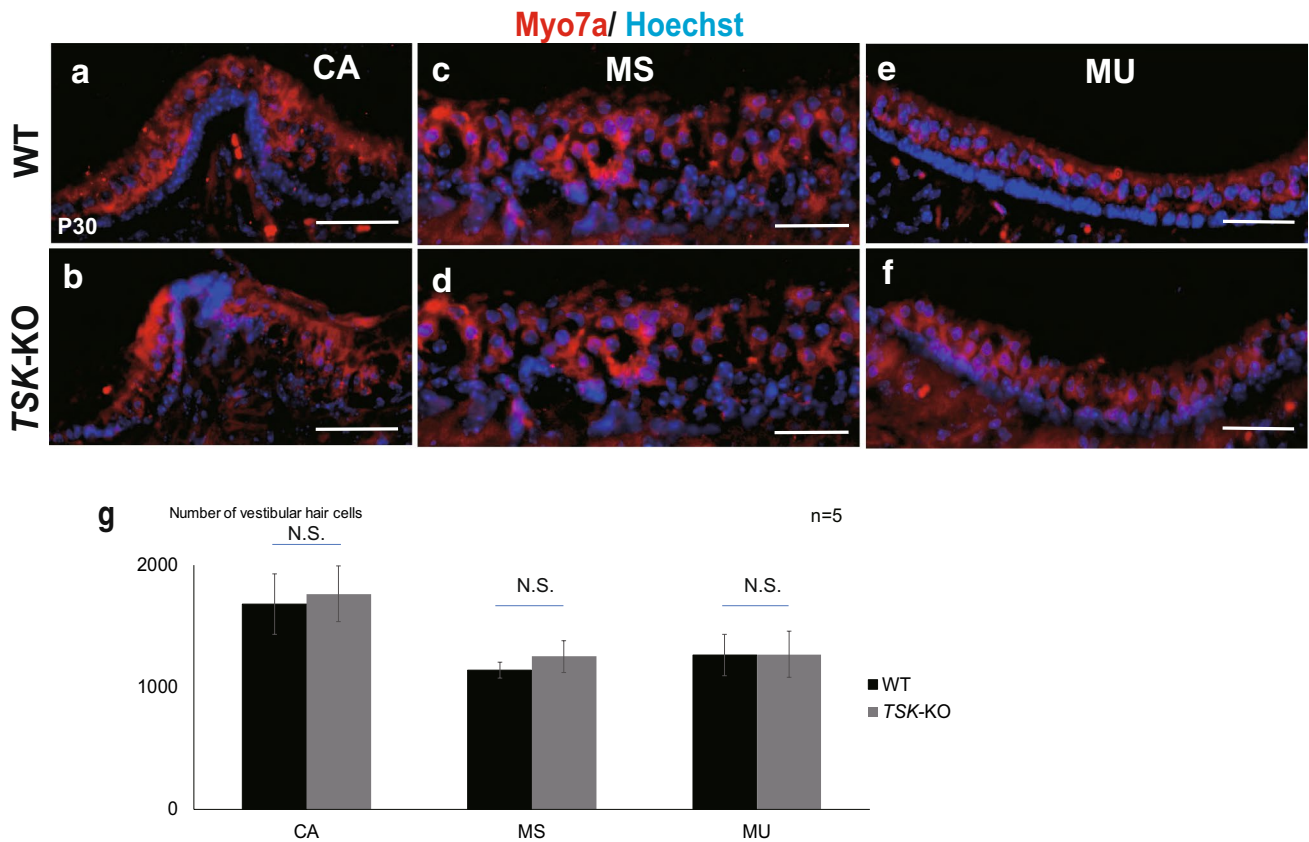


Fig. 3 Number of vestibular hair cells in the vestibules at P30 in WT and *TSK-KO* mice. Representative immunostaining images of CA (**a**, **b**), MS (**c**, **d**), and MU (**e**, **f**), using the anti-Myo7a antibody, counterstained with Hoechst in WT (top) and *TSK-KO* (bottom) mice. **g** The

number of vestibular hair cells did not significantly differ between the groups in all regions ($n=5$; $P=0.29$ at CA, $P=0.06$ at MS, $P=0.48$, N.S., not significant). CA, crista ampullae; MS, maculae saccule; MU, macula utricule. Scale bar: 100 μ m

(Fig. 5d), whereas it was similarly localized in *TSK-KO* mice, albeit at slightly decreased levels (Fig. 5e). The results of the quantitative PCR analysis showed that there were no significant differences in *Bmp4* mRNA expression between the WT and *TSK-KO* mice (Fig. 5f, $P=0.28$). FGF10 was weakly detected in the WT mice vestibules (Fig. 5f); in the *TSK-KO* mice, it was enhanced in the MS, C-SC duct, ASC, LSC, and PA (Fig. 5g). DLX5 was slightly upregulated in the MS, C-SC duct, ASC, LSC, and PA in the vestibular epithelium of *TSK-KO* compared with that in WT (Fig. 5h, i). We used ISH and IHC, as ISH did not work in this experiment. For the same reasons, we separated fluorescence and DAB.

***TSK-KO* suppressed SOX2 and thinly spread *Bmp4*, but did not change *Wnt2b* in the prosensory regions**

SOX2 was detected by immunolabeling in the prosensory regions, such as the MS, MU, and LA in WT mice, but was decreased in the *TSK-KO* mice at E13.5 (Fig. 6a, b). *Sox2* mRNA in the prosensory regions of vestibules was significantly decreased in the absence of TSK (Fig. 6c, $P=0.04$). *Wnt2b* mRNA was not detected in the prosensory regions of either group (Fig. 6d, e). In WT mice, *Bmp4* mRNA was detected in the MS, MU, and LA (Fig. 6f), whereas in the *TSK-KO* mice, it was more widely distributed (Fig. 6g). Negative controls of *Wnt2b*, *Bmp4*, DLX5, FGF10, and SOX2 staining are shown in Online Resource 5 Supplementary Information.

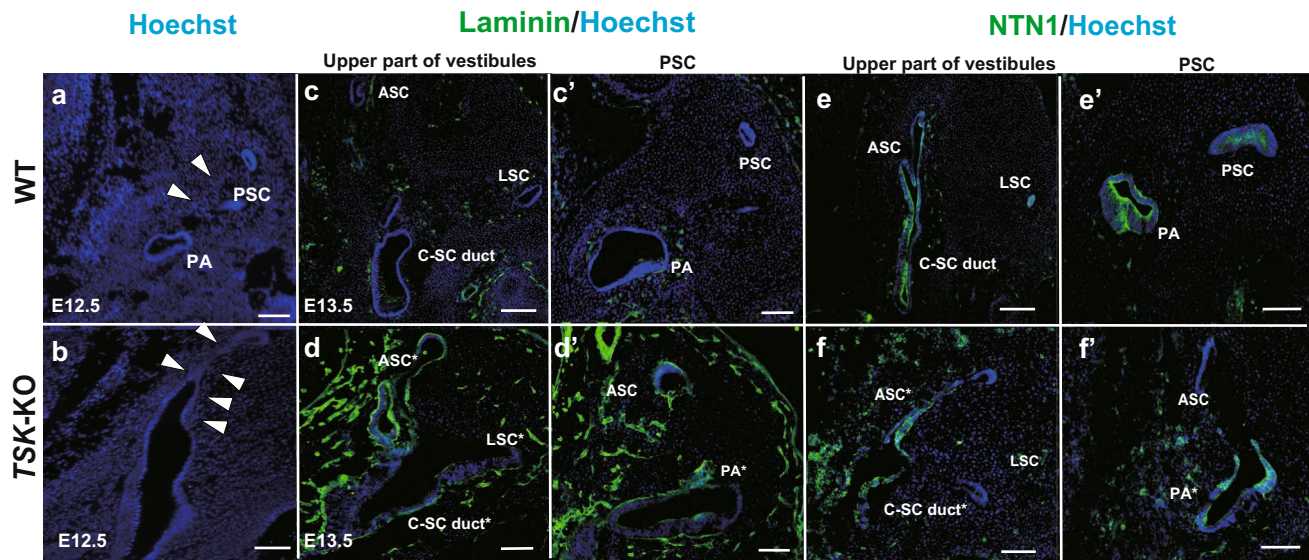


Fig. 4 Loss of TSK signaling blocks fusion plate formation. **a, b** Morphology of mouse vestibules at E12.5. **a** The vestibular epithelial cells were lost after fusion plate formation in the PSC outpocketing in WT mice. **b** In *TSK-KO* mice, the vestibular epithelial cells remained in the PSC outpocketing. The arrowheads indicate the regions of the PSC outpocketing. **c–d'** At E13.5, immunohistochem-

istry showed that the laminin expression was upregulated (asterisks). **e–f'** At E13.5, immunohistochemistry showed that NTN1 was slightly upregulated around the vestibular epithelium (asterisks). C-SC duct, common semicircular canal duct; ASC, anterior semicircular canal; LSC, lateral semicircular canal; PSC, posterior semicircular canal; PA, posterior ampullae. Scale bar: 50 μ m

Discussion

Appropriate morphogenesis of the inner ear SCs requires the precise regulation of cellular proliferation, EMT, and fusion of epithelial plates (Wu and Kelley 2012). Understanding the coupling of signaling pathways and the transcription factor network activity of cell behavior and the physical force that affects these morphogenetic events is one of the major challenges in understanding inner ear development (Alsina and Whitfield 2017). As TSK has been previously shown to inhibit Bmp (Ohta et al. 2004), Wnt (Dellett et al. 2012; Ohta et al. 2011), and FGF signaling (Morris et al. 2007; Uejima et al. 2010), and it is a factor associated with the matrix metalloproteinase signaling cascade (Ni et al. 2014; Pietraszek-Gremplewicz et al. 2019), we investigated its roles in the development of semicircular canals and vestibular sensory regions.

TSK is required for posterior semicircular canal formation and normal gait performance

Our study revealed that PSC was defective and gait performance deteriorated in *TSK-KO* mice (Online Resource 1, 3 and 4). The malformation of PSC has been described in several human diseases (Higashi et al. 1992; Irie et al.

1990; Wiener-Vacher et al. 1999; Wright et al. 1985); however, abnormal gait has not been reported to date. Studies in animal models of these disorders (Baynash et al. 1994; Motohashi et al. 1994; Owens et al. 2005) have not reported gait performance and vestibular function. Clinically, patients with PSC dehiscence syndrome, secondary to the absence of a bony covering of the PSC, suffer from chronic vestibular symptoms (Di Lella et al. 2007). Therefore, we speculate that bilateral PSC defects caused a loss of rotational and balance senses, resulting in an abnormal gait.

TSK is crucial for the local disruption of the basement membrane and fusion plate formation

During semicircular duct formation, the epithelial walls destined to form fusion plates first become thinner, and then the cells lose their epithelial morphology due to the local disruption of the underlying basement membrane (Martin and Swanson 1993). Our study revealed that upregulated laminin expression around the vestibular epithelium in the *TSK-KO* mice resulted in basement membrane disruption and fusion plate formation failure (Fig. 7a). However, the NTN1 level was slightly higher in the *TSK-KO* vestibules. Both NTN1 and TSK bind to secreted frizzled (Fzd)-related

proteins (Bovolenta et al. 2008), which modulate Wnt and Bmp signaling. TSK also inhibits the local production of matrix metalloproteinases (Ni et al. 2014; Pietraszek-Gremplewicz et al. 2019). Therefore, we propose that NTN1 and TSK function together to induce proliferation of the periotic mesenchyme.

TSK participates in a resorption cascade including epithelial–mesenchymal signaling

Our data showed that in the absence of TSK, the *Wnt2b* level was higher in the C-SC duct, the origin of posterior canal rims. We found that the *TSK*-KO mice showed slightly decreased *Bmp4* expression “thinly spread” throughout the vestibules, indicating that *Bmp4* is expressed in not only the original region of expression, but also in other vestibular epithelium; however, it was not upregulated. We speculated that TSK regulated Wnt and Bmp signaling and induced PSC morphogenesis.

FGF10 expression was upregulated in the entire vestibular epithelium of the *TSK*-KO mice. As FGF10 is an extracellular protein with a high affinity to heparin, we hypothesize that FGF10 secreted from the developing crista affects the neighboring prospective canal epithelium via proteins with heparin-binding domains, such as NTN1.

TSK is not required in the development of the sensory regions of vestibules

We observed that SOX2 was suppressed in the vestibular prosensory regions at the early embryonic stage. Generally, SOX2 promotes the generation of hair cells via the upregulation of the transcription factor Atoh1, which is involved in generating sensory hair cells (Dabdoub et al. 2008; Kempfle et al. 2016; Puligilla et al. 2010; Zheng and Gao 2000). However, we did not observe any decrease in the number of vestibular hair cells in the CA, MS, or MU in the *TSK*-KO mice.

Hair cells consist of the cell body and stereocilia. They are susceptible to Atoh1, which dose-dependently controls the stereocilia formation and organization (Jahan et al. 2013). Previous studies have suggested that the level and duration of SOX2 expression affect stereocilia formation and length (Jahan et al. 2013; Pan et al. 2013). Thus, the vestibular hair cells of the *TSK*-KO mice may have abnormal stereocilia although we did not observe them.

Conclusions

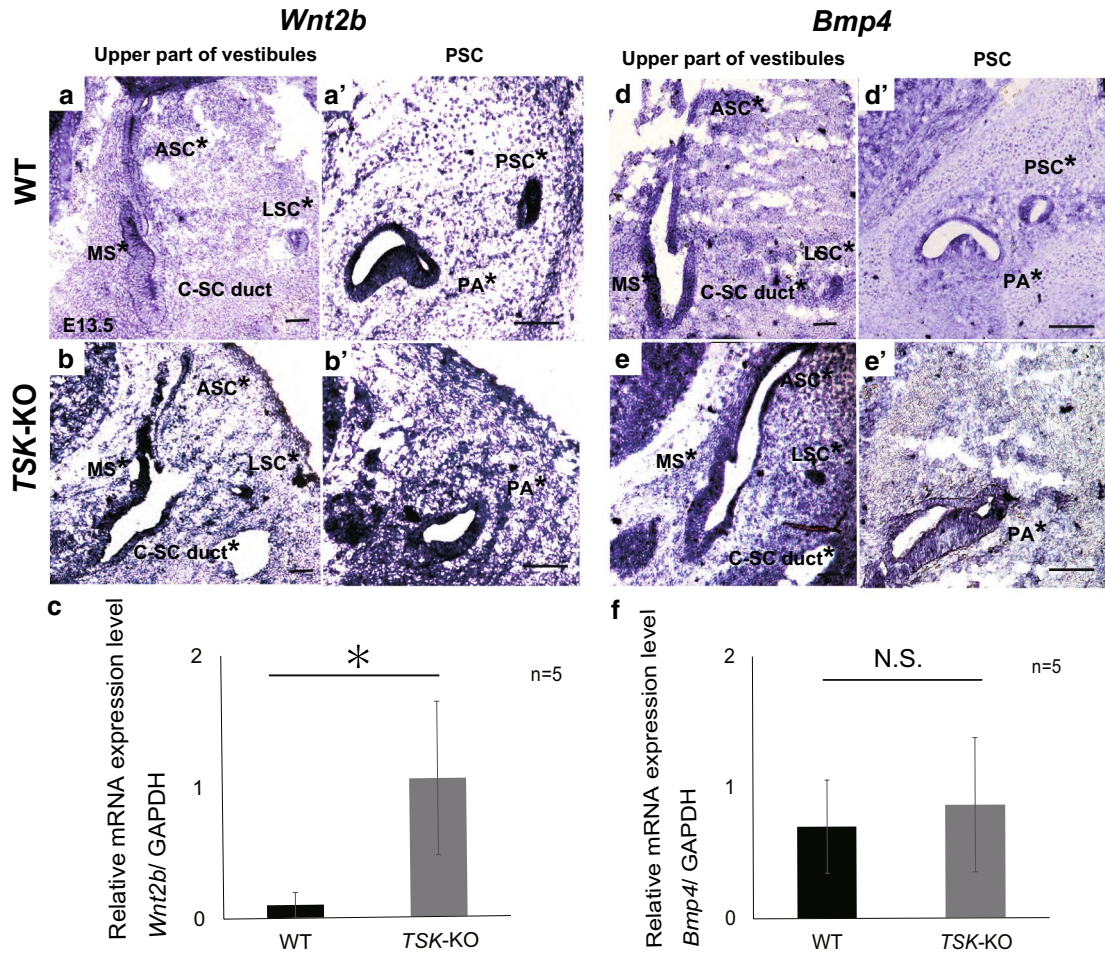
We confirmed that TSK is expressed in the sensory and non-sensory regions of the ear during inner ear morphogenesis and is required for the development of PSC and gait in mice. Its deletion caused disequilibrium and complete PSC defect in line with the *Wnt2b* level, redistributing *Bmp4* and enhancing FGF10 signaling. Moreover, NTN1-dependent resorption through the otic epithelium of the semicircular duct outpocketing could not form normal fusion plates in the *TSK* mutant. Our results suggest a new morphogenetic role of TSK in the development of the mouse vestibular system. This study had a few limitations. First, we did not investigate the stereocilia of the vestibular hair cells. Second, we did not observe other sensory regions, such as the vestibular ganglion cells and the central nervous system. Finally, the relationship between sensory signaling during development and the non-sensory elements of the semicircular canal system was not investigated.

Supplementary Information The online version contains supplementary material available at <https://doi.org/10.1007/s12079-021-00627-1>.

Acknowledgements We thank Ms. Miho Kataoka for technical assistance and all laboratory members for their valuable help.

Author's contributions TM performed the experiments, analyzed the data, and wrote the manuscript. TM, IN, and KO designed the experiments and supervised the study.

Nonsensory



Nonsensory

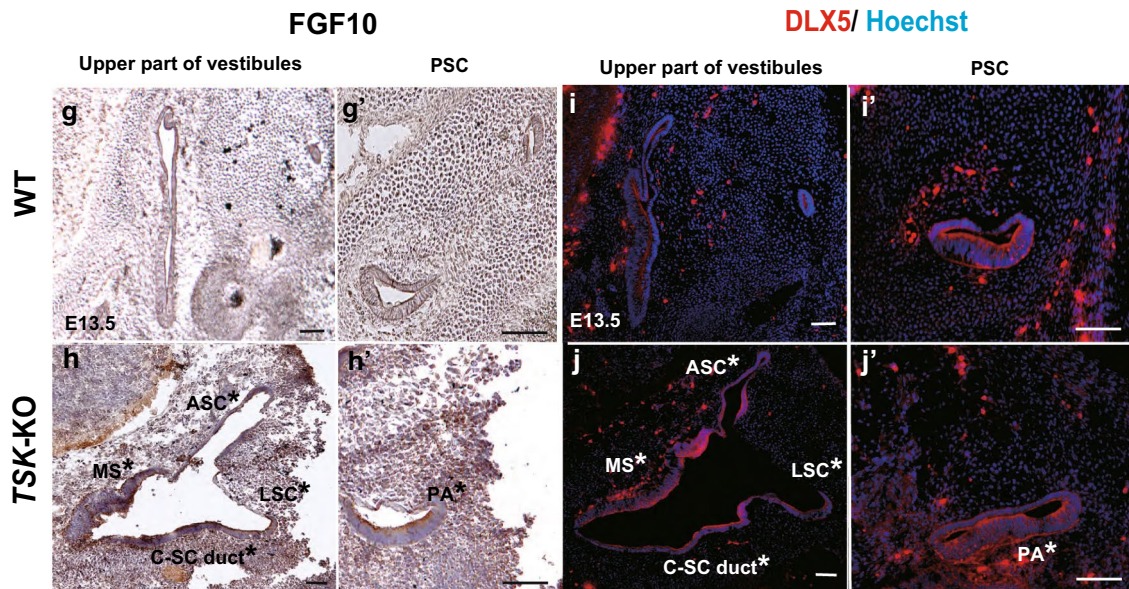


Fig. 5 Dynamic vestibular gene expression in the non-sensory regions in the WT and *TSK-KO* mice. **a** *Wnt2b* was detected by in situ hybridization in the MS, LSC, and ASC of the upper part of vestibules (**a**) and PA and PSC of PSC levels (**a'**) in WT mice. **b** In *TSK-KO* mice, *Wnt2b* was detected in the MS, C-SC duct, LSC, and ASC of the upper part of vestibules (**b**) and PA and PSC of PSC levels (**b'**). **c** *Wnt2b* mRNA expression significantly increased in *TSK-KO* vestibules compared with that in WT vestibules ($P=0.01$). **d** *Bmp4* mRNA was detected by in situ hybridization in the MS, C-SC duct, LSC, and ASC of the upper part of vestibules (**d**) and PSC of PSC levels (**d'**) in WT mice. **e** In *TSK-KO* mice, *Bmp4* mRNA was detected in the non-sensory vestibules, including the C-SC duct, LSC, and ASC of the upper part of vestibules (**e**) and PSC levels (**e'**), but at slightly decreased levels. **f** There were no significant differences in *Bmp4* mRNA expression of whole vestibule tissues between WT and *TSK-KO* mice ($P=0.28$). **g–h'** In *TSK-KO* mice, FGF10 was upregulated compared with that in the WT vestibules. **i–j'** In *TSK-KO* mice, DLX5 was slightly upregulated compared with that in WT vestibules. C-SC duct, common semicircular canal duct; ASC, anterior semicircular canal; LSC, lateral semicircular canal; PSC, posterior semicircular canal; PA, posterior ampullae. Scale bar: 50 μ m

Funding This research received no specific grant from any funding agency in the public, commercial, or not-for-profit sectors.

Availability of data and materials All data are available upon reasonable request from the corresponding author.

Declarations

Conflict of interest The authors declare no conflicts of interest.

References

- Ahmad SAI, Anam MB, Ito N, Ohta K (2018) Involvement of Tsukushi in diverse developmental processes. *J Cell Commun Signal* 12:205–210. <https://doi.org/10.1007/s12079-018-0452-8>
- Ahmad SAI, Anam MB, Istiaq A, Ito N, Ohta K (2020) Tsukushi is essential for proper maintenance and terminal differentiation of mouse hippocampal neural stem cells. *Dev Growth Differ* 62:108–117. <https://doi.org/10.1111/dgd.12649>
- Alsina B, Whitfield TT (2017) Sculpting the labyrinth: morphogenesis of the developing inner ear. *Semin Cell Dev Biol* 65:47–59. <https://doi.org/10.1016/j.semcdb.2016.09.015>
- Baynash AG, Hosoda K, Giaid A, Richardson JA, Emoto N, Hammer RE, Yanagisawa M (1994) Interaction of endothelin-3 with endothelin-B receptor is essential for development of epidermal melanocytes and enteric neurons. *Cell* 79:1277–1285. [https://doi.org/10.1016/0092-8674\(94\)90018-3](https://doi.org/10.1016/0092-8674(94)90018-3)
- Bovolenta P, Esteve P, Ruiz JM, Cisneros E, Lopez-Rios J (2008) Beyond Wnt inhibition: new functions of secreted Frizzled-related proteins in development and disease. *J Cell Sci* 121:737–746. <https://doi.org/10.1242/jcs.026096>
- Chang W, Lin Z, Kulesha H, Hebert J, Hogan BLM, Wu DK (2008) *Bmp4* is essential for the formation of the vestibular apparatus that detects angular head movements. *PLOS Genet* 4:e1000050. <https://doi.org/10.1371/journal.pgen.1000050>
- Dabdoub A, Puligilla C, Jones JM, Fritsch B, Cheah KSE, Pevny LH, Kelley MW (2008) SOX2 signaling in prosensory domain specification and subsequent hair cell differentiation in the developing cochlea. *Proc Natl Acad Sci USA* 105:18396–18401. <https://doi.org/10.1073/pnas.0808175105>
- Dellett M, Hu W, Papadaki V, Ohnuma S (2012) Small leucine rich proteoglycan family regulates multiple signalling pathways in neural development and maintenance. *Dev Growth Differ* 54:327–340. <https://doi.org/10.1111/j.1440-169X.2012.01339.x>
- Di Lella F, Falcioni M, Piazza P (2007) Dehiscence of posterior semicircular canal. *Otol Neurotol* 28:280–281. <https://doi.org/10.1097/01.mao.0000231592.64972.5b>
- Fekete DM, Homburger SA, Waring MT, Riedl AE, Garcia LF (1997) Involvement of programmed cell death in morphogenesis of the vertebrate inner ear. *Development* 124:2451–2461. <https://doi.org/10.1242/dev.124.12.2451>
- Fernagut PO, Diguët E, Labattu B, Tison F (2002) A simple method to measure stride length as an index of nigrostriatal dysfunction in mice. *J Neurosci Methods* 113:123–130. [https://doi.org/10.1016/S0165-0270\(01\)00485-X](https://doi.org/10.1016/S0165-0270(01)00485-X)
- Higashi K, Matsuki C, Sarashina N (1992) Aplasia of posterior semicircular canal in Waardenburg syndrome type II. *J Otolaryngol* 21:262–264
- Hocking AM, Shinomura T, McQuillan DJ (1998) Leucine-rich repeat glycoproteins of the extracellular matrix. *Matrix Biol* 17:1–19. [https://doi.org/10.1016/S0945-053X\(98\)90121-4](https://doi.org/10.1016/S0945-053X(98)90121-4)
- Hossain M, Ahmed G, Naser IB, Shinmyo Y, Ito A, Riyadh MA, Felemban A, Song X, Ohta K, Tanaka H (2013) The combinatorial guidance activities of draxin and Tsukushi are essential for forebrain commissure formation. *Dev Biol* 374:58–70. <https://doi.org/10.1016/j.ydbio.2012.11.029>
- Huang SM, Mishina YM, Liu S et al (2009) Tankyrase inhibition stabilizes axin and antagonizes Wnt signalling. *Nature* 461:614–620. <https://doi.org/10.1038/nature08356>
- Irie K, Ogata H, Mitsudome A (1990) CT findings of the temporal bones in Waardenburg's syndrome. *No to Hattatsu* 22:241–246
- Ito A, Shinmyo Y, Abe T, Oshima N, Tanaka H, Ohta K (2010) Tsukushi is required for anterior commissure formation in mouse brain. *Biochem Biophys Res Commun* 402:813–818. <https://doi.org/10.1016/j.bbrc.2010.10.127>
- Ito N, Riyadh MA, Ahmad SAI, Hattori S, Kanemura Y, Kiyonari H, Abe T, Furuta Y, Shinmyo Y, Kaneko N, Hirota Y, Lupo G, Hatakeyama J, Abdulhaleem MFA, Anam MB, Yamaguchi T, Takeo T, Takebayashi H, Takebayashi M, Oike Y, Nakagata N, Shimamura K, Holtzman MJ, Takahashi Y, Guillemot F, Miyakawa K, Sawamoto K, Ohta K (2021) Dysfunction of the proteoglycan Tsukushi causes hydrocephalus through altered neurogenesis in the subventricular zone. *Sci Transl Med* 13:eaay7896
- Jahan I, Pan N, Kersigo J, Fritsch B (2013) Beyond generalized hair cells: molecular cues for hair cell types. *Hear Res* 297:30–41. <https://doi.org/10.1016/j.heares.2012.11.008>
- Kempfle JS, Turban JL, Edge ASB (2016) SOX2 in the differentiation of cochlear progenitor cells. *Sci Rep* 6:23293. <https://doi.org/10.1038/srep23293>
- Kiernan AE, Pelling AL, Leung KKH, Tang ASP, Bell DM, Tease C, Lovell-Badge R, Steel KP, Cheah KSE (2005) SOX2 is required for sensory organ development in the mammalian inner ear. *Nature* 434:1031–1035. <https://doi.org/10.1038/nature03487>
- Kiernan AE, Xu J, Gridley T (2006) The notch ligand JAG1 is required for sensory progenitor development in the mammalian inner ear. *PLOS Genet* 2:e4. <https://doi.org/10.1371/journal.pgen.0020004>
- Lang H, Bever MM, Fekete DM (2000) Cell proliferation and cell death in the developing chick inner ear: spatial and temporal patterns. *J Comp Neurol* 417:205–220. [https://doi.org/10.1002/\(SICI\)1096-9861\(20000207\)417:2%3c205::AID-CNE6%3e3.0.CO;2-Y](https://doi.org/10.1002/(SICI)1096-9861(20000207)417:2%3c205::AID-CNE6%3e3.0.CO;2-Y)

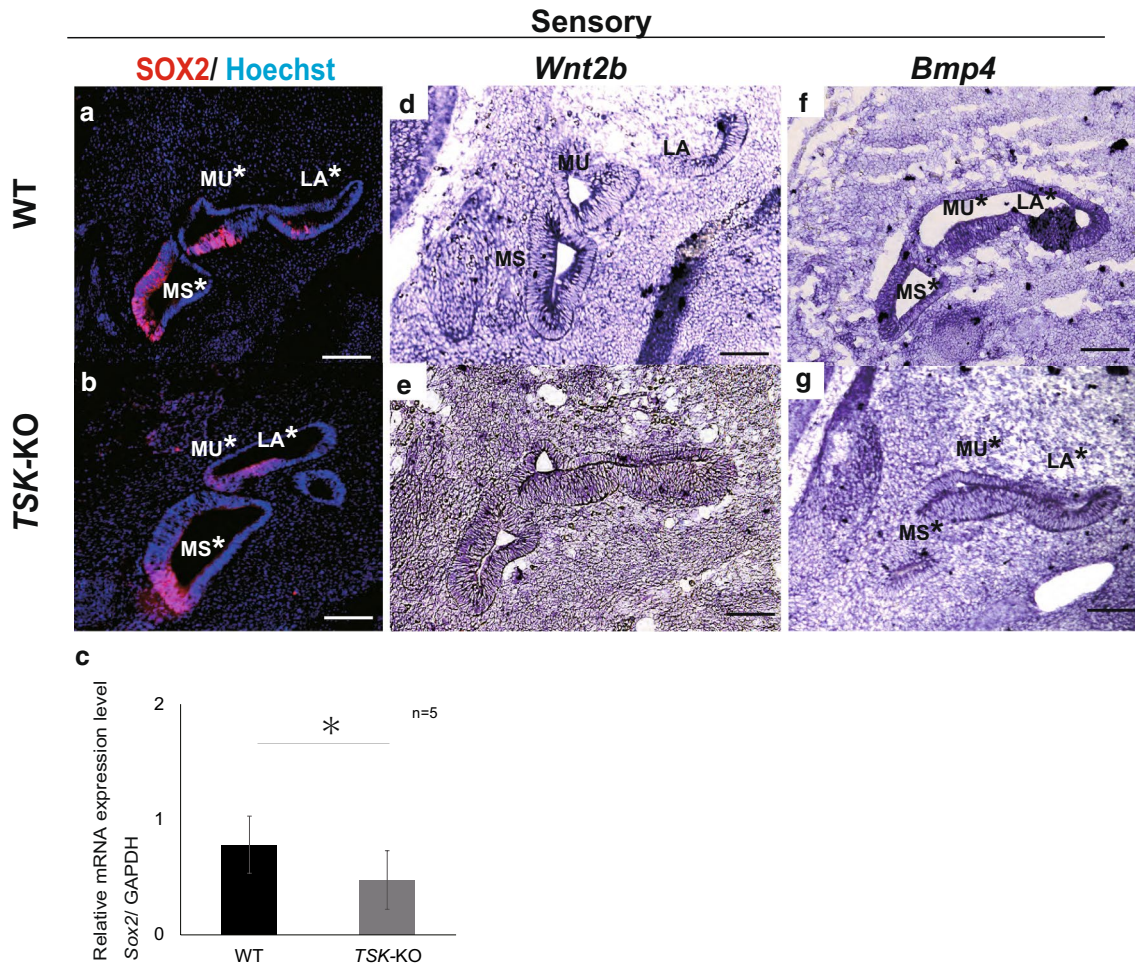


Fig. 6 Dynamic vestibular gene expression in the prosensory regions in WT and *TSK-KO* mice. **a, b** SOX2 expression decreased in *TSK-KO* mice at E13.5. **c** *Sox2* mRNA expression significantly decreased in the absence of TSK ($P=0.04$) compared with that in WT. **d, e**

Wnt2b mRNA was not detected by in situ hybridization in both groups. **f** *Bmp4* mRNA was detected by in situ hybridization in the MS, MU, and LA in WT mice. **g** *Bmp4* mRNA was thinly spread by in situ hybridization in *TSK-KO* mice. Scale bar: 50 μ m

- Langman J, Sadler TW (2008) Langman's medical embryology, 12th edn. Wolters Kluwer Health/Lippincott Williams & Wilkins, Philadelphia
- Li H, Corrales CE, Wang Z, Zhao Y, Wang Y, Liu H, Heller S (2005) BMP4 signaling is involved in the generation of inner ear sensory epithelia. *BMC Dev Biol* 5:16. <https://doi.org/10.1186/1471-213X-5-16>
- Martin P, Swanson GJ (1993) Descriptive and experimental analysis of the epithelial remodellings that control semicircular canal formation in the developing mouse inner ear. *Dev Biol* 159:549–558. <https://doi.org/10.1006/dbio.1993.1263>
- Merline R, Schaefer RM, Schaefer L (2009) The matricellular functions of small leucine-rich proteoglycans (SLRPs). *J Cell Commun Signal* 3:323–335. <https://doi.org/10.1007/s12079-009-0066-2>
- Miwa T, Minoda R, Ishikawa Y, Kajii T, Orita Y, Ohyama T (2019) Role of Dach1 revealed using a novel inner ear-specific Dach1-knockdown mouse model. *Biol Open* 8:bio043612. <https://doi.org/10.1242/bio.043612>
- Miwa T, Ohta K, Ito N, Hattori S, Miyakawa T, Takeo T, Nakagata N, Song WJ, Minoda R (2020) Tsukushi is essential for the development of the inner ear. *Mol Brain* 13:29. <https://doi.org/10.1186/s13041-020-00570-z>

- Morris SA, Almeida AD, Tanaka H, Ohta K, Ohnuma S (2007) Tsukushi modulates Xnr2:FGF and BMP signaling: regulation of *Xenopus* germ layer formation. *PLoS ONE* 2:e1004. <https://doi.org/10.1371/journal.pone.0001004>
- Motohashi H, Hozawa K, Oshima T, Takeuchi T, Takasaka T (1994) Dysgenesis of melanocytes and cochlear dysfunction in mutant microphthalmia (*mi*) mice. *Hear Res* 80:10–20. [https://doi.org/10.1016/0378-5955\(94\)90003-5](https://doi.org/10.1016/0378-5955(94)90003-5)
- Ni GX, Li Z, Zhou YZ (2014) The role of small leucine-rich proteoglycans in osteoarthritis pathogenesis. *Osteoarthr Cartil* 22:896–903. <https://doi.org/10.1016/j.joca.2014.04.026>
- Niimori D, Kawano R, Felemban A, Niimori-Kita K, Tanaka H, Ihn H, Ohta K (2012) Tsukushi controls the hair cycle by regulating TGF- β 1 signaling. *Dev Biol* 372:81–87. <https://doi.org/10.1016/j.ydbio.2012.08.030>
- Ohta K, Lupo G, Kuriyama S, Keynes R, Holt CE, Harris WA, Tanaka H, Ohnuma SI (2004) Tsukushi functions as an organizer inducer by inhibition of BMP activity in cooperation with chordin. *Dev Cell* 7:347–358. <https://doi.org/10.1016/j.devcel.2004.08.014>
- Ohta K, Kuriyama S, Okafuji T, Gejima R, Ohnuma S, Tanaka H (2006) Tsukushi cooperates with VGI to induce primitive streak

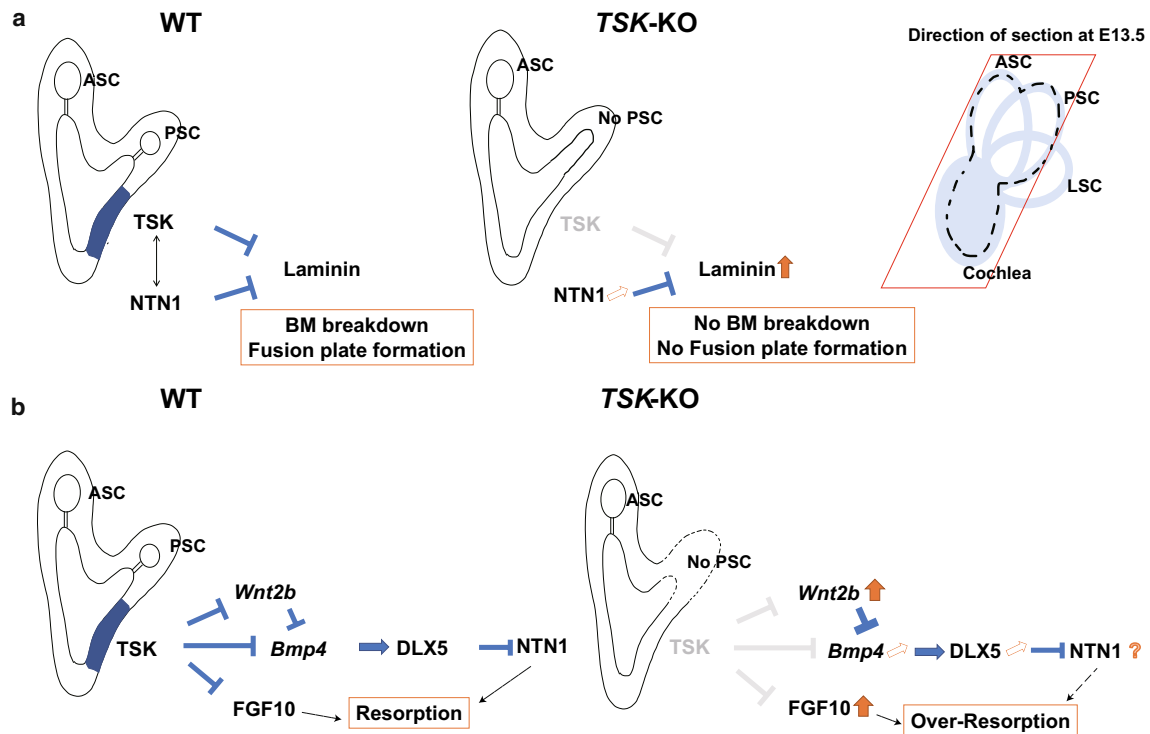


Fig. 7 Proposed mechanism of TSK function in the vestibules. **a** Schema of basement membrane breakdown and fusion plate formation. We propose that NTN1 and TSK function together to induce proliferation in the periotic mesenchyme. **b** Schema of resorption by

epithelial–mesenchymal signaling. We speculate that TSK regulates Wnt, Bmp, and FGF signaling and functions with DLX5 and NTN1 to induce PSC morphogenesis

- and Hensen's node formation in the chick embryo. *Development* 133:3777–3786. <https://doi.org/10.1242/dev.02579>
- Ohta K, Ito A, Kuriyama S, Lupu G, Kosaka M, Ohnuma SI, Nakagawa S, Tanaka H (2011) Tsukushi functions as a Wnt signaling inhibitor by competing with *Wnt2b* for binding to transmembrane protein Frizzled4. *Proc Natl Acad Sci USA* 108:14962–14967. <https://doi.org/10.1073/pnas.1100513108>
- Ohuchi H, Yasue A, Ono K, Sasaoka S, Tomonari S, Takagi A, Itakura M, Moriyama K, Noji S, Nohno T (2005) Identification of cis-element regulating expression of the mouse *Fgf10* gene during inner ear development. *Dev Dyn* 233:177–187. <https://doi.org/10.1002/dvdy.20319>
- Ohyama T, Basch ML, Mishina Y, Lyons KM, Segil N, Groves AK (2010) BMP signaling is necessary for patterning the sensory and nonsensory regions of the developing mammalian cochlea. *J Neurosci* 30:15044–15051. <https://doi.org/10.1523/JNEUROSCI.3547-10.2010>
- Owens SE, Broman KW, Wiltshire T, Elmore JB, Bradley KM, Smith JR, Southard-Smith EM (2005) Genome-wide linkage identifies novel modifier loci of aganglionosis in the *Sox10*Dom model of Hirschsprung disease. *Hum Mol Genet* 14:1549–1558. <https://doi.org/10.1093/hmg/ddi163>
- Pagedar NA, Wang W, Chen DHC, Davis RR, Lopez I, Wright CG, Alagramam KN (2006) Gene expression analysis of distinct populations of cells isolated from mouse and human inner ear FFPE tissue using laser capture microdissection—a technical report based on preliminary findings. *Brain Res* 1091:289–299. <https://doi.org/10.1016/j.brainres.2006.01.057>
- Pan W, Jin Y, Chen J, Rottier RJ, Steel KP, Kiernan AE (2013) Ectopic expression of activated notch or SOX2 reveals similar and unique roles in the development of the sensory cell progenitors in the mammalian inner ear. *J Neurosci* 33:16146–16157. <https://doi.org/10.1523/JNEUROSCI.3150-12.2013>
- Pauley S, Wright TJ, Pirvola U, Ornitz D, Beisel K, Fritzsche B (2003) Expression and function of FGF10 in mammalian inner ear development. *Dev Dyn* 227:203–215. <https://doi.org/10.1002/dvdy.10297>
- Pietraszek-Gremplewicz K, Karamanou K, Niang A, Dauchez M, Belloy N, Maquart FX, Baud S, Brézillon S (2019) Small leucine-rich proteoglycans and matrix metalloproteinase-14: key partners? *Matrix Biol* 75–76:271–285. <https://doi.org/10.1016/j.matbio.2017.12.006>
- Postigo AA (2003) Opposing functions of ZEB proteins in the regulation of the TGFbeta/BMP signaling pathway. *EMBO J* 22:2443–2452. <https://doi.org/10.1093/emboj/cdg225>
- Puligilla C, Dabdoub A, Brenowitz SD, Kelley MW (2010) SOX2 induces neuronal formation in the developing mammalian cochlea. *J Neurosci* 30:714–722. <https://doi.org/10.1523/JNEUROSCI.3852-09.2010>
- Rakowiecki S, Epstein DJ (2013) Divergent roles for Wnt/β-catenin signaling in epithelial maintenance and breakdown during semicircular canal formation. *Development* 140:1730–1739. <https://doi.org/10.1242/dev.092882>
- Rao J, Pfeiffer MJ, Frank S, Adachi K, Piccini I, Quaranta R, Araúz-Bravo M, Schwarz J, Schade D, Leidel S, Schöler HR, Seeböhm G, Greber B (2016) Stepwise clearance of repressive roadblocks drives cardiac induction in human ESCs. *Cell Stem Cell* 18:341–353. <https://doi.org/10.1016/j.stem.2015.11.019>
- Salminen M, Meyer BI, Bober E, Gruss P (2000) Netrin 1 is required for semicircular canal formation in the mouse inner ear. *Development* 127:13–22

- Schaefer L, Iozzo RV (2008) Biological functions of the small leucine-rich proteoglycans: from genetics to signal transduction. *J Biol Chem* 283:21305–21309. <https://doi.org/10.1074/jbc.R800020200>
- Schneider CA, Rasband WS, Eliceiri KW (2012) NIH Image to ImageJ: 25 years of image analysis. *Nat Methods* 9:671–675. <https://doi.org/10.1038/nmeth.2089>
- Shibata S, Miwa T, Wu HH, Levitt P, Ohyama T (2016a) Hepatocyte growth factor–c-MET signaling mediates the development of nonsensory structures of the Mammalian Cochlea and hearing. *J Neurosci* 36:8200–8209. <https://doi.org/10.1523/JNEUROSCI.4410-15.2016>
- Shibata SB, Ranum PT, Moteki H, Pan B, Goodwin AT, Goodman SS, Abbas PJ, Holt JR, Smith RJH (2016b) RNA interference prevents autosomal-dominant hearing loss. *Am J Hum Genet* 98:1101–1113. <https://doi.org/10.1016/j.ajhg.2016.03.028>
- Takeda H, Miwa T, Kim MY, Choi BY, Orita Y, Minoda R (2019) Prenatal electroporation-mediated gene transfer restores Slc26a4 knock-out mouse hearing and vestibular function. *Sci Rep* 9:17979. <https://doi.org/10.1038/s41598-019-54262-3>
- Uejima A, Amano T, Nomura N, Noro M, Yasue T, Shiroishi T, Ohta K, Yokoyama H, Tamura K (2010) Anterior shift in gene expression precedes anteriormost digit formation in amniote limbs. *Dev Growth Differ* 52:223–234. <https://doi.org/10.1111/j.1440-169X.2009.01161.x>
- Vervoort R, Ceulemans H, Van Aerscht L, D’Hooge R, David G (2010) Genetic modification of the inner ear lateral semicircular canal phenotype of the Bmp4 haplo-insufficient mouse. *Biochem Biophys Res Commun* 394:780–785. <https://doi.org/10.1016/j.bbrc.2010.03.069>
- Werb Z, Chin JR (1998) Extracellular matrix remodeling during morphogenesis. *Ann NY Acad Sci* 857:110–118. <https://doi.org/10.1111/j.1749-6632.1998.tb10111.x>
- Wiener-Vacher SR, Amanou L, Denise P, Narcy P, Manach Y (1999) Vestibular function in children with the CHARGE association. *Arch Otolaryngol Head Neck Surg* 125:342–347. <https://doi.org/10.1001/archotol.125.3.342>
- Wright CG, Brown OE, Meyerhoff WL, Rutledge JC (1985) Inner ear anomalies in two cases of trisomy 18. *Am J Otolaryngol Neck Surg* 6:392–404. [https://doi.org/10.1016/S0196-0709\(85\)80018-1](https://doi.org/10.1016/S0196-0709(85)80018-1)
- Wu DK, Kelley MW (2012) Molecular mechanisms of inner ear development. *Cold Spring Harb Perspect Biol* 4:a008409. <https://doi.org/10.1101/cshperspect.a008409>
- Yano K, Washio K, Tsumanuma Y, Yamato M, Ohta K, Okano T, Izumi Y (2017) The role of Tsukushi (TSK), a small leucine-rich repeat proteoglycan, in bone growth. *Regen Ther* 7:98–107. <https://doi.org/10.1016/j.reth.2017.08.001>
- Zheng JL, Gao WQ (2000) Overexpression of Math1 induces robust production of extra hair cells in postnatal rat inner ears. *Nat Neurosci* 3:580–586. <https://doi.org/10.1038/75753>

Publisher’s Note Springer Nature remains neutral with regard to jurisdictional claims in published maps and institutional affiliations.